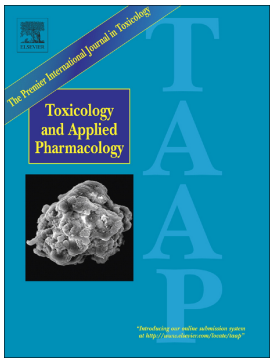

Zebrafish (Danio rerio) model as an early stage screening tool to study the biodistribution and toxicity profile of doxorubicin-loaded mixed micelles

María Natalia Calienni, Maximiliano Cagel, Jorge Montanari, Marcela A. Moretton, Maria Jimena Prieto, Diego A. Chiappetta, Silvia del Valle Alonso

PII: S0041-008X(18)30332-6
DOI: doi:10.1016/j.taap.2018.07.019
Reference: YTAAP 14343

To appear in: *Toxicology and Applied Pharmacology*

Received date: 11 May 2018
Revised date: 16 July 2018
Accepted date: 18 July 2018

Please cite this article as: María Natalia Calienni, Maximiliano Cagel, Jorge Montanari, Marcela A. Moretton, Maria Jimena Prieto, Diego A. Chiappetta, Silvia del Valle Alonso , Zebrafish (Danio rerio) model as an early stage screening tool to study the biodistribution and toxicity profile of doxorubicin-loaded mixed micelles. Ytaap (2018), doi:10.1016/j.taap.2018.07.019

Zebrafish (*Danio rerio*) model as an early stage screening tool to study the biodistribution and toxicity profile of doxorubicin-loaded mixed micelles

María Natalia Calienni[1#], Maximiliano Cagel[2,3#], Jorge Montanari[1], Marcela A. Moretton[2,3], Maria Jimena Prieto[1], Diego A. Chiappetta[2,3], Silvia del Valle Alonso[1*]

[1]Laboratory of Biomembranes - GBEyB (IMBICE, CCT-La Plata, CONICET), Departamento de Ciencia y Tecnología, National University of Quilmes, Bernal, Argentina. [2]Universidad de Buenos Aires. Facultad de Farmacia y Bioquímica. Cátedra de Tecnología Farmacéutica I. Buenos Aires, Argentina. [3]Consejo Nacional de Investigaciones Científicas y Técnicas (CONICET).

[#] Both authors contributed equally to this work.

*Corresponding author

Dr. Silvia del Valle Alonso

[1]Laboratory of Biomembranes - GBEyB (IMBICE, CCT-La Plata, CONICET), Departamento de Ciencia y Tecnología, National University of Quilmes, Bernal, Argentina.

Roque Sáenz Peña 352,

Bernal, (1876), Provincia de Buenos Aires

Argentina

Email: salonso@unq.edu.ar

Phone/Fax: +54-11-4365-7100 ext.5625

Abstract

Doxorubicin (DOX) hydrochloride is a powerful anthracycline antibiotic used for the treatment of various types of malignancies, particularly ovarian and metastatic breast cancer. However, DOX presents severe side effects, such as hepatotoxicity, nephrotoxicity, dose-limiting myelosuppression, brain damage and cardiotoxicity. A liposomal formulation, Doxil®, was approved by the FDA, which has managed to reduce the number of cardiac events in patients with metastatic breast cancer. However, in comparison to free DOX, Doxil® has not shown significant improvements regarding survival. We have previously designed DOX-loaded mixed micelles (MMDOX) composed of D-α-tocopheryl polyethylene glycol 1000 succinate (TPGS) and Tetronic® T1107. To assess the potential toxic effects of this novel formulation, in this work the zebrafish (*Danio rerio*) model was used to evaluate its *in vivo* toxicity and teratogenicity. This study evaluated and compared the effects of DOX exposure from different formulations (free DOX, MMDOX and Doxil®) on the swimming activity, morphological alterations, cardiac rhythm, lethality rate and DOX biodistribution. MMDOX showed lower lethal effects, morphological alterations and neurotoxic effects than the free drug. This study shows the potential of the MMDOX to be an effective DOX-delivery system because it could reduce the side effects.

Keywords: *Danio rerio*, wild-type zebrafish, nanotoxicity, mixed micelles, doxorubicin

1. Introduction

The antineoplastic drugs used in the chemotherapeutic treatment do not differentiate between healthy and cancerous cells, generating a great variety of adverse effects. One of the drugs of choice as a chemotherapeutic agent is the doxorubicin (DOX) hydrochloride, a powerful anthracycline antibiotic used for more than four decades for the treatment of various types of malignancies, particularly ovarian and metastatic breast cancer (Mohan and Rapoport, 2010). However, due to its short biological lifespan and nonspecific distribution, DOX presents severe side effects, such as hepatotoxicity, nephrotoxicity, dose-limiting myelosuppression, brain damage and significant cardiotoxicity (Damodar et al., 2014; Kuznetsov et al., 2011; Rizk et al., 2017), limiting its maximum doses of application. A pegylated liposomal formulation known as Doxil® was approved by the Food and Drug Agency of the United States (FDA) in 1995 (Cagel et al., 2017b), which has managed to reduce the number of cardiac events in patients with metastatic breast cancer. However, in comparison to free DOX, Doxil® has not shown significant improvements regarding survival (O'Brien et al., 2004). This performance is due mainly to the poor cellular uptake and slower DOX release from the liposomes (O'Brien et al., 2004). This latter is responsible for the reduction of adverse effects, while the first is a consequence of the presence of polyethylene-glycol (PEG) on the surface of this kind of nanoformulations. This process known as "pegylation" strongly inhibits the cell penetration (Duggan and Keating, 2011; Zhao et al., 2016).

In this context, we have recently designed and characterized DOX-loaded mixed micelles (MMDOX) composed of D-α-tocopheryl polyethylene glycol 1000

succinate (TPGS) and Tetronic® T1107. We demonstrated an enhanced *in vitro* antitumoral efficacy of these MMDOX *versus* Doxil® in breast (MDA-MB-231) and ovarian (SKOV-3) human cancer cell lines (Cagel et al., 2017a). In our case, TPGS was used as an interesting alternative to replace PEG and improve the cellular drug internalization in comparison to Doxil®, as it has been stated that TPGS may inhibit P-glycoprotein (P-gp), the efflux pump that mediates multidrug resistance in tumor cells (Zhang et al., 2012).

Taking into account these promising *in vitro* results, the future investigations will be focused on the evaluation of the *in vivo* antitumoral efficacy of the MMDOX *versus* Doxil®. Nevertheless, additional studies to assess the potential toxic effects of micellar formulations are still needed. Zebrafish model (*Danio rerio*) is increasingly accepted and validated for the *in vivo* toxicity and teratogenicity testing of colloidal nano-drug delivery systems (Li et al., 2017). Its advantages as an intermediate model prior to *in vivo* studies in mammals are -among others- the high genetic homology with humans, the molecular and physiological similarities with mammals, the *ex utero* growth, the ability to perform high-throughput screenings due to the high number of fertilized eggs after spawning, and its fast development that allows to study the establishment of the principal organ systems during the first week (Lee et al., 2017). Regarding antitumoral drugs, the zebrafish model allows to determinate parameters such as lethal dose, acute toxicity, teratogenicity and specific-organ toxicity, in particular of the heart and the nervous system (Calienni et al., 2017b; Raldúa and Piña, 2014). Also, the transparent body of zebrafish allows studying the biodistribution of actives and drug delivery systems by diverse imaging techniques (Lillo et al., 2018). In the particular case of DOX, some

nanotechnological platforms have been recently assayed in zebrafish model to evaluate some of these parameters (Ang et al., 2017; Chen et al., 2017; Gao et al., 2017; Sun et al., 2016).

In this work, with the aim of comparing the *in vivo* toxicity of different DOX formulations (DOX, empty mixed micelles -MM-, MMDOX, and Doxil®) in zebrafish, the swimming activity, morphological alterations, cardiac rhythm, lethality rate, and biodistribution were studied.

2. Materials and methods

2.1. Materials

Tetronic® 1107 (T1107, MW ~15.0 kDa, 70 wt% PEO) was a gift of BASF® (Argentina). TPGS (MW ~1513 g/mol) was purchased from Eastman Chemical Company (USA), sodium deoxycholate (NaDC) was purchased from Riedel-de Häen® (Germany). Doxorubicin hydrochloride (99.9%) was purchased from LKM Laboratories (Argentina). Doxil® was purchased from Raffo Laboratories (Argentina). Sodium carboxymethylcellulose was from Fluka-BioChemika (Sigma-Aldrich, Argentina) and sucrose from Anedra (Buenos Aires, Argentina). Agar-agar was from Laboratorios Britania S.A. (Buenos Aires, Argentina). All other reagents used were from analytical grade.

2.2. Methods

2.2.1. Preparation of mixed micelles

Mixed colloidal systems were prepared as previously described (Cagel et al., 2017a). Briefly, T1107 and TPGS (weight ratio 1:3) were dispersed in distilled

water at room temperature to get a final polymer concentration of 2% w/v. Samples were equilibrated at 25°C for 24 h before use.

2.2.2. Preparation and characterization of DOX-loaded mixed micelles

The encapsulation of DOX within the mixed micellar systems was performed as previously described (Cagel et al., 2017a). Briefly, a DOX-sodium deoxycholate (NaDC) complex was obtained by dissolving DOX hydrochloride (50 mg) in distilled water (10 ml) and adding NaDC (90 mg) to the solution under magnetic stirring (2 h). Then, the insoluble DOX-NaDC complex suspension was centrifuged (5600 rpm, 10 min, 20°C, Refrigerated Centrifuge Combi 514R, Hanil Science Industrial Co., Korea), the precipitate was re-dispersed with distilled water (10 ml) and homogenized with vortex (Vortex Mixer Wizard, Velp Scientifica, Italy).

Afterward, the complex suspension was added in excess to the mixed micellar dispersions and left under magnetic stirring for 2 h. Then, dispersions were filtered (0.45 µm acetate cellulose filters, Microclar, Argentina) and stored at 4°C. DOX quantification was performed UV–vis spectrophotometry (λ: 500 nm, UV-260, UV–vis Recorder Spectrophotometer, Shimadzu, Japan) in N,N-Dimethylformamide at room temperature, employing a calibration curve between 5 and 63 µg/ml in N,N-Dimethylformamide. Assays were done in triplicate, and the results were expressed as the average ± standard deviation (SD).

The average hydrodynamic diameter (D_h) and micellar size distribution of the MM and MMDOX (2% w/v polymer concentration) were measured by Dynamic Light Scattering (DLS) (scattering angle of θ =173° to the incident beam,

Zetasizer Nano-ZSP, Malvern Instruments, United Kingdom) at 25°C. Samples were filtered (0.45 µm acetate cellulose filters, Microclar, Argentina) and equilibrated for 5 minutes prior the analysis. The results were expressed as the average of three measurements ± standard deviation (SD).

2.2.3. Zebrafish husbandry and embryo collection

Wild-type adult zebrafish (*Danio rerio*) were kept in glass tanks (height: 20 cm x width: 27 cm x length: 40 cm, and 16.4 liters of water), at 26 ± 1ºC under a 14/10 hour of light/dark cycle. Females were separated in different batches with three males for stimulating, for each 12 females. The density of fish in each tank was one fish/liter of water. Each group of females was paired each 15 days. Fish were fed with dry food (TetraMin PRO®) three times per day and once with live brine shrimp (*Artemia persimilis*) (VitaFish, Argentina). Water was constantly aerated, maintained at pH 7.0 – 8.0 with a hardness of 50-100 mg/l (2º to 6º), dissolved oxygen 5 mg/l, conductivity 300-1000 µs, ammonium < 0.02 ppm, nitrites < 0.1 ppm and nitrates < 5-10 ppm.

Zebrafish embryos were obtained by natural pair-wise mating in our aquarium. Sexually mature females and males (8–12 months old) were selected the evening before spawning, breeding pairs in a ratio of three females for two males. They were transferred to glass tanks (height: 20 cm x width: 20 cm x length: 40 cm, and 12 liters of water), specially designed to maintain females and males separately overnight at 28 ± 1ºC, and to prevent the embryos from cannibalism. The first light stimulus after the dark cycle induced the spawning when they were put together. The collected embryos after fertilization were conserved in E3 medium (NaCl 0.29 g/l, KCl 0.012 g/l, $CaCl_2$ 0.036 g/l and

$MgSO_4$ 0.039 g/l in deionized water, and 50 ppb methylene blue) and maintained at 28 ± 1ºC with a cycle of 14/10 h of light/dark up to the end of the experiments.

2.2.4. Developmental toxicity determination on zebrafish

In vivo toxicological studies were carried out on larvae of wild-type zebrafish between 4 and 7 days post-fecundation (dpf). For all experiments, three embryos of one-dpf were placed in the wells of a 96-well microplate with 225 µl of E3 medium until 4 dpf (larval stage). At 4 dpf, 25 µl of the 10-fold concentrated serial dilutions in E3 medium of DOX, MM, MMDOX, and Doxil® were added to each well. For all cases, the same concentration of free or encapsulated DOX (12.5-200 µg/ml), or the corresponding polymer concentration for MM (125-2000 µg/ml), was evaluated to compare the different conditions. Larvae in the E3 medium were used as a control of non-treated animals. The treatment solution was not removed during the study. Fig. 1 depicts the experimental design for the toxicological evaluation. For each biological replicate, adults from different batches were paired.

2.2.5. Survival rate

The mortality rate of larvae was determined at 4, 24, 48 and 72 hours post-incubation (hpi). The absence of heartbeat was considered the criterion of dead. A total of eight larvae per condition were monitored over time, in duplicate.

2.2.6. Determination of the heart rate and morphological changes

The heart rate and morphological changes were assessed at 72 hpi as described by Calienni et al., (Calienni et al., 2017b). Briefly, four larvae per condition were immobilized with sodium carboxymethylcellulose to be photographed and filmed (Microsoft LifeCam Studio camera coupled to a trinocular microscope Nikon SMZ800, Japan). The number of beats over 15 seconds was counted and reported as percent of heart rate with respect to the untreated control. Morphological endpoints of toxicity such as larval eye area, rostrocaudal length, spinal cord length, uninflated swim bladder, arched body, tissue ulceration and pericardial edema, were analyzed with ImageJ Software (US NIH, Bethesda, Maryland, USA). Both studies were carried out in duplicate.

2.2.7. Measurement of the spontaneous swimming activity

Swimming activity of larvae was determined with a WMicrotracker device (Designplus SRL, Buenos Aires, Argentina) as in previous works (Calienni et al., 2017a). Briefly, the activity of larvae in the 96-well microplate was recorded for 15 min at room temperature at 4, 24, 48 and 72 hpi. Swimming activity was determined as the number of interruptions of the infrared microbeam arrangement of the device. A total of eight wells per condition were measured in triplicate and results were relativized to the untreated control and reported as the percent of swimming activity for each time.

2.2.8. Biodistribution

The biodistribution of DOX was studied in larvae incubated with a concentration of free drug, MMDOX and Doxil® that corresponded to 50 µg/ml of DOX. Larvae treated with MM and non-treated larvae were included as controls. Five larvae

per condition were anesthetized with a tricaine methanesulfonate 0.3 g/l solution at 72 hpi and fixed with 4% w/v paraformaldehyde in phosphate buffer at 4°C overnight. The larvae were embedded and oriented in blocks of agar-sucrose for imaging by confocal laser scanning microscopy (CLSM) equipped with a He–Ne laser (excitation 543 nm) (Olympus FluoView FV300). The sampling speed was 8.0 µs/pixel, and the quality of images obtained was 12 bits/pixel. The photomultiplier voltage was 800 V. Images were analyzed by ImageJ software.

2.2.9. Ethics Statement

All animal procedures were performed in strict accordance with International Guidelines for animal care and maintenance. The protocols were approved by the Institutional Committee for the Care and Use of Laboratory Animals and the Ethics Committee of the National University of Quilmes (CICUAL-UNQ 013-15), Buenos Aires, Argentina.

2.2.10. Statistical analysis

Data obtained from *in vivo* assays are presented as the mean ± SD or the standard error of the mean (SEM) and analyzed by one-way analysis of variance (ANOVA) and multiple comparisons test of Dunnett. Each sample was compared to the control. GraphPad Prism version 6.0 was used to conduct all statistical analyses. Only values with $p < 0.05$ were accepted as significant.

3. Results and discussion

3.1. Characterization of the mixed micelles

In the present study, an amphiphilic block copolymer known as T1107 and a water-soluble derivative of natural vitamin E known as TPGS were used to prepare the mixed micellar formulation. T1107 is a 4-armed branched copolymer that belongs to the poloxamine family of block copolymers and presents sensitiveness to both temperature and pH (Chiappetta et al., 2008). On the other hand, TPGS was chosen for its properties as P-gp inhibitor and its *in vitro* and *in vivo* anticancer activity (Neophytou et al., 2014).

As nano-sized carriers, polymeric micelles are well-known to be dynamic systems. In this way, changes on micellar aggregation behavior and sample polydispersion could be found not only after drug encapsulation, but also micellar dilution and associated to environmental factors (pH, temperature, ion strength) (Owen et al., 2012). The D_h and micellar size distribution of the MM and MMDOX (2% w/v total polymer concentration) were measured by DLS at 25 ºC. Micellar size of the MM was slightly higher (13.2 ± 0.2 nm) in comparison to the MMDOX (10.7 ± 0.2 nm). Besides, both preparations exhibited a unimodal and narrow size distribution (Fig. 2), as demonstrated by the low polydispersity index (PDI) values of 0.044 ± 0.014 and 0.239 ± 0.010 for the MM and MMDOX, respectively. These findings suggested that after drug encapsulation within the core, DOX altered the aggregation pattern of TPGS:T1107 mixture leading to a slight shift to lower average D_h. Similar behavior was observed for nelfinavir-loaded TPGS micelles (Moretton et al., 2014) and rifampicin-loaded poly(epsilon-caprolactone)-b-PEG-b-poly(epsilon-caprolactone) polymeric micelles (Moretton et al., 2010).

The D_h and size distribution of Doxil® were also measured by DLS at 25ºC. This commercial nanoformulation presented a D_h of 85.1 ± 0.8 nm, and exhibited a

unimodal distribution (Fig. 2) with a PDI value of 0.114 ± 0.002. These values were in good agreement with previous data (Cagel et al., 2017b).

3.2. *In vivo* toxicity on zebrafish larvae

As mentioned before, zebrafish studies have been established as a preclinical intermediate model system for the evaluation of efficacy and toxicity of novel drug carriers (Liu et al., 2013). In our case, this study aimed to compare the toxicity *in vivo* of different DOX formulations: free DOX, MMDOX, Doxil®, and MM as a preliminary step to further studies in a mammal model. The incubation at 4 dpf allows not only the observation of developmental neurological damage, but also corresponds to the transition from an inactive to a fully inflated swim bladder, the development of sensory systems and organs such as liver and heart are functional at 5 dpf (De Esch et al., 2012). Larvae can live until 7 dpf supported by nutrients stored in the yolk sac without exogenous feeding (He et al., 2013).

3.2.1. Survival rate

The mortality of zebrafish larvae after exposure to different concentrations of DOX, MMDOX, Doxil®, and MM was determined after 4, 24, 48 and 72 hpi (corresponding to 4-7 dpf) (Fig. 3). Free DOX presented the highest rate of mortality in comparison to the other treatments. The encapsulation of DOX into MM reduced the lethal effect of the drug. After 4 hpi, the concentration that corresponds to 100 µg/ml of DOX induced the death of the 100% of larvae treated with the free drug, while MMDOX produced a 75% of death (Fig. 3a). After 24 hpi, free drug induced an 80% of mortality of individuals treated with 50

µg/ml, whereas MMDOX induced a 50% of death for the same concentration (Fig. 3b). After 48 hpi, free drug killed the 88% of larvae exposed to 50 µg/ml, while MMDOX did not increase the rate of death significantly (Fig. 3c). Empty MM did not cause lethal effects even at maximum concentration after 72 hpi, which would indicate that the active would be the main responsible of the toxic effect. The commercial liposomal formulation Doxil® was toxic only at the maximum concentration since 48 hpi (Fig. 3c), reaching a 50% of mortality at 72 hpi (Fig. 3d). Therefore, it was necessary a 4-fold higher concentration of Doxil® in comparison to MMDOX to produce a 50% of death after 72 hpi. This differential effect could be related to the lower release of DOX encapsulated into Doxil® than into MMDOX observed in our previous *in vitro* study (Cagel et al., 2017a). For all treatments, there was no significant difference in mortality compared with the control group at concentrations less than 25 µg/ml of DOX. Chang et al., 2014 observed a similar rate of death in larvae of zebrafish treated with free DOX at 3 dpf during 96 h (Chang et al., 2014).

3.2.2. Alterations of the heart rate

As cardiotoxicity is one of the most severe side-effects of DOX, we also examined the effect of the different formulations on zebrafish heart rate after 72 hpi (Fig. 4). Zebrafish has demonstrated to be a good model for the study of cardiovascular diseases (Asnani and Peterson, 2014; Gut et al., 2017). Despite there are anatomic differences between the zebrafish heart and mammalian heart, several studies have highlighted similarities in the genes and regulatory networks (Asnani and Peterson, 2014). Particularly, Huang et al., 2007 showed

that DOX induces similar cardiac defects in zebrafish as in mammals (Huang et al., 2007).

In this study, larvae were treated during 72 h at 4 dpf, period in which the heart is in the final development process (De Esch et al., 2012). Larvae exposed to concentrations higher than 100 µg/ml of free DOX and MMDOX were all dead. Free DOX induced a significant increase in the heart rate when larvae were exposed to concentrations higher than 25 µg/ml. MMDOX did not present statistically significant alterations, but it is evident that there was an increase in the dispersion of data for larvae treated with concentrations higher than 25 µg/ml. The range of concentration of adverse effect of MMDOX was similar to that of DOX. This effect could be related to the release of DOX from MMDOX during the period of exposition as we had previously observed (Cagel et al., 2017a). On the other hand, Doxil® showed alteration in the heart rate with respect to the control only when larvae were exposed to 200 µg/ml. It is known that Doxil® has a slower release than MMDOX (Cagel et al., 2017a). Thus the poor release of DOX from Doxil® could be related to the lower cardiotoxicity observed in this study. Even though limiting the toxicity could be an advantage, on the other hand, this slow release is also responsible of a poor *in vitro* antitumor activity (Cagel et al., 2017a). The MM did not present alteration of the heart rate for any concentration tested (corresponding to the concentration of polymers present in the MMDOX).

3.2.3. Morphological changes

Toxicity of nanoformulations is frequently associated with malformations in zebrafish embryo and larva (Zhou et al., 2016). In this case, morphological

endpoint parameters were analyzed after 72 hpi for each treatment. No alterations regarding the eye area, rostrocaudal and spinal cord length were observed. In addition, larvae did not present signals of pericardial edema as observed in embryos upon DOX treatment (Huang et al., 2007; Yang et al., 2011). The main adverse effect was the presence of an uninflated swim bladder. The treatment with free DOX was the most toxic, presenting morphological alterations for all concentration tested (Table 1). Larvae treated with DOX 12.5 and 25 µg/ml only presented uninflated swim bladder in 25% and 62.5% of individuals, respectively. Besides, treatment with DOX 50 µg/ml induced the presence of uninflated swim bladder in the 87.5%, arched body and ulcerated tissue in the 12.5% of the individuals studied. Larvae treated with 12.5 µg/ml of MMDOX did not present alterations, whereas larvae treated with 25 and 50 µg/ml presented uninflated swim bladder (37.5%) and arched body (12.5%). No determinations of morphological alterations could be carried out in larvae exposed to concentrations higher than 100 µg/ml of DOX and MMDOX because of their damaged condition. Treatments with MM and Doxil® did not present any morphological endpoint of toxicity studied.

3.2.4. Spontaneous swimming activity

Measurement of the alteration of the spontaneous swimming activity allows the prediction of neurotoxic effects in zebrafish larvae (Selderslaghs et al., 2013). High or low activity with respect to the control could be indicative of adverse effects. Larvae were exposed to DOX, MMDOX, Doxil®, and MM at 4 dpf and swimming activity was measured at 4, 24, 48 and 72 hpi (4, 5, 6 and 7 dpf). Data are shown in Fig. 5. The treatment with free DOX produced a significant

increase of swimming activity at low concentrations (12.5 and 25 µg/ml) since 24 hpi and a significant decrease for high concentrations (100 and 200 µg/ml) since 4 hpi. On the other hand, only larvae exposed high concentrations of MMDOX (100 and 200 µg/ml) presented a significative decrease in the activity with respect to the control since 4 hpi. No significant alterations in the swimming activity of larvae were observed under treatment with MM and Doxil®. Regarding Doxil®, this apparent absence of neurotoxicity could be related again to the low rate of drug release from the liposome (Cagel et al., 2017a). The profile of behavior of larvae treated with MMDOX was similar to those treated with DOX only at high concentrations, while the MM did not alter the swimming activity. Therefore, the potential neurotoxic effect observed in zebrafish larvae would be associated with DOX but not with the vehicle.

The low rate of activity of larvae treated with 100 and 200 µg/ml of MMDOX and DOX could be mainly related to the high rate of mortality. While the alteration in the swimming activity at low concentrations of free DOX could be evidence of neurotoxicity, and could also be related to the swim bladder affection and the alteration in the heart rate observed. The behavior of larvae treated with 50 µg/ml of DOX could be a result of both effects observed for lower and higher concentrations and was observed as a movement similar to the untreated control. These results are in accordance with previous works which showed that DOX induced cytotoxic effects *in vitro* in primary cultured neurons, and *in vivo* produced neurotoxic effects in the brain of mice and rat (Kosoko et al., 2017; Moruno-Manchon et al., 2018). Even though DOX poorly crosses the blood-brain barrier (BBB) in humans, it still arrives at the brain at doses sufficient to cause neurotoxicity (Kesler and Blayney, 2016).

Therefore, the encapsulation of DOX into MMDOX reduced its neurotoxic effects, being this an interesting strategy to take advantage of when employing a nanotechnological platform. Nevertheless, more exhaustive studies should be carried out to confirm the neurotoxic effect of the free DOX on zebrafish.

3.2.5. Biodistribution

CLSM was performed to detect differences in the localization of the DOX on larvae after 72 hpi with DOX, MMDOX, and Doxil®. The zebrafish transparency during the larval stage and the fluorescent properties of DOX provide advantages for *in vivo* visualization and could serve as a valuable tool for identifying tissue-specific distribution. DOX could be tracked even when is encapsulated into nanocarriers using fluorescence-based techniques without any other fluorescence labels (Zou et al., 2017).

As could be seen in Fig. 6, DOX was found within the lumen of the gut of larvae after 72 hpi with DOX, MMDOX and Doxil® (in all cases the concentration of DOX corresponded to 50 µg/ml). This accumulation could be related to the oral uptake of the formulation, although it is not the only route of entry as internalization also could happen by the gills and by skin absorption (He et al., 2013).

However, when larvae were observed by CLSM a more generalized distribution could be seen (Fig. 7). The free DOX and MMDOX showed a more generalized distribution on the larvae than Doxil®. A similar distribution was observed by Yao et al., 2017 on larvae treated with free DOX between 4-6 dpf (Yao et al., 2017). In all cases, the highest fluorescent intensity was found in the gut, which corresponded with the accumulation of the DOX-loaded formulations and the

drug observed by bright-field microscopy. As expected no fluorescence was observed in larvae treated with MM and non-treated control.

The BBB function of zebrafish is developed between 3-10 dpf (Fleming et al., 2013), while it has a functional gastrointestinal barrier with a mature intestinal epithelium at 5 dpf (Ng et al., 2005). For this reason, during the period of study, the BBB was not fully formed and would allow DOX and formulations to arrive in the brain. As mentioned above, the internalization of the different formulations may occur by oral uptake, skin and gills absorption. In all cases, the DOX (free or encapsulated) was able to enter in the blood-circulation and to reach a generalized distribution. However, a more exhaustive analysis of the biodistribution should be carried out.

Despite the good therapeutic efficacy of DOX, the free drug presents severe side effects, due to its non-specific distribution (Damodar et al., 2014). For this reason, in 1995 the FDA approved Doxil®, a drug-controlled release PEGylated liposomal formulation, whose main achievement in clinical stages was the reduction of the cardiotoxic effects of DOX. However, this system did not significantly improve the anticancer efficacy (Cagel et al., 2017b), fact that could be related to the very low release rate of the drug, even when it reaches the target. Moreover, it presents other adverse effects inherent to these PEGylated liposomes. On the one hand, as a result of their increased circulation time in human plasma, they produce a grade 2/3 desquamating dermatitis, known as hand-foot syndrome or palmar-plantar erythrodysesthesia (Cagel et al., 2017b), that affects the quality of life of the patient and may require a reduction of dose or even a temporary interruption of the treatment. On the other hand, it has

been studied that the components of Doxil® particularly generate a complement-activation-related-pseudo-allergy (CARPA), that involves flushing and shortness of breath (Cagel et al., 2017b). Therefore, the aim of encapsulating DOX into MM was to control the biodistribution and modify its pharmacokinetics, with a nanotechnological platform that favors the release once reached the target and increases the therapeutic effect. In a previous work, we developed and characterized a MMDOX formulation with an improved *in vitro* anticancer effect at significantly lower concentrations of DOX, in comparison to both Doxil® and the free drug (Cagel et al., 2017a). To compare the cytotoxic effect, we have determined the IC50 values of the nanoformulations and free DOX in two human cancer cell lines. The IC50 is the concentration of the tested formulations that kills 50% of the cells, being this predictive of the degree of cytotoxic effect. In general, the lower the value, the more cytotoxic is the compound. In the case of the ovarian cancer cell line (SKOV-3), the IC50 of the MMDOX (0.17 µg/ml) resulted in 2.4- and 3.4-fold lower than those of Doxil® (0.41 µg/ml) and free DOX (0.58 µg/ml), respectively. In the case of the breast cancer cell line (MDA-MB-231), the IC50 of the DOX-loaded mixed micellar (0.11 µg/ml) formulation was 6.9- and 1.5-fold lower than the values of Doxil® (0.76 µg/ml) and free DOX (0.16 µg/ml), respectively (Cagel et al., 2017a). Overall, these results showed that our MMDOX clearly improved the *in vitro* anticancer effect against ovarian and breast cancer cell lines, in comparison to Doxil® and free DOX. It is worth stressing that the concentrations used in the toxicity and survival rate assays of the current study are markedly higher than the mentioned IC50 values previously reported by our group (Cagel et al., 2017a). In the present work, we observed that the encapsulation of DOX into

MMDOX reduced the main toxic side effects of the free drug on zebrafish model. Particularly, *in vivo* cardiotoxicity experiments carried out in zebrafish showed that MMDOX exhibited less cardiotoxic effect than free DOX. Considering our previous *in vitro* anticancer results and the current *in vivo* studies in zebrafish, the mixed micellar formulation appears to be an interesting and potential nanotechnological platform as an alternative DOX-delivery system to be evaluated in an *in vivo* mammal cancer model.

4. Conclusion

In this paper, we have evaluated and compared the main toxic side effects of free DOX and DOX-loaded nanoformulations on the preclinical zebrafish model. The encapsulation of DOX into the mixed micelles reduced the lethal effect, the morphological alterations and the neurotoxic effects of the drug. The DOX-associated toxicity of the mixed micellar formulation exhibited a substantial decrease compared with that of free DOX. However, regarding cardiotoxic effects, the three formulations with DOX did alter the heart rate in the larvae. On the view of these results with MMDOX in this intermediate model, further studies could be performed in an *in vivo* mammal cancer model to assess its antitumoral efficacy and safety.

Acknowledgments

This work was supported by the Universidad Nacional de Quilmes (PUNQ 1388/15), Consejo Nacional de Investigaciones Científicas y Técnicas (CONICET) and Universidad de Buenos Aires (Grant UBACyT 20020130200038BA). Diego A. Chiappetta, Jorge Montanari, Marcela A.

Moretton, María Jimena Prieto and Silvia del Valle Alonso are members of CONICET, Argentina. Maximiliano Cagel and María Natalia Calienni acknowledge fellowship from CONICET Argentina.

References

Ang, C.Y., Tan, S.Y., Teh, C., Lee, J.M., Wong, M.F.E., Qu, Q., Poh, L.Q., Li, M., Zhang, Y., Korzh, V., Zhao, Y., 2017. Redox and pH Dual Responsive Polymer Based Nanoparticles for In Vivo Drug Delivery. Small 13. https://doi.org/10.1002/smll.201602379

Asnani, A., Peterson, R.T., 2014. The zebrafish as a tool to identify novel therapies for human cardiovascular disease. Dis. Model. Mech. 7, 763–767. https://doi.org/10.1242/dmm.016170

Cagel, M., Bernabeu, E., Gonzalez, L., Lagomarsino, E., Zubillaga, M., Moretton, M.A., Chiappetta, D.A., 2017a. Mixed micelles for encapsulation of doxorubicin with enhanced in vitro cytotoxicity on breast and ovarian cancer cell lines versus Doxil®. Biomed. Pharmacother. 95, 894–903. https://doi.org/10.1016/j.biopha.2017.09.006

Cagel, M., Grotz, E., Bernabeu, E., Moretton, M.A., Chiappetta, D.A., 2017b. Doxorubicin: nanotechnological overviews from bench to bedside. Drug Discov. Today. https://doi.org/10.1016/j.drudis.2016.11.005

Calienni, M.N., Feas, D.A., Igartúa, D.E., Chiaramoni, N.S., Alonso, S. del V., Prieto, M.J., 2017a. Nanotoxicological and teratogenic effects: A linkage between dendrimer surface charge and zebrafish developmental stages. Toxicol. Appl. Pharmacol. 337, 1–11. https://doi.org/10.1016/j.taap.2017.10.003

Calienni, M.N., Temprana, C.F., Prieto, M.J., Paolino, D., Fresta, M., Tekinay, A.B., Alonso, V., Montanari, J., 2017b. Nano-formulation for topical treatment of precancerous lesions : skin penetration , in vitro , and in vivo toxicological evaluation.

Chang, C., Wu, S.L., Zhao, X.D., Zhao, C.T., Li, Y.H., 2014. Developmental toxicity of doxorubicin hydrochloride in embryo-larval stages of zebrafish. Biomed. Mater. Eng. 24, 909–916. https://doi.org/10.3233/BME-130885

Chen, J., Wu, Q., Luo, L., Wang, Y., Zhong, Y., Dai, H. Bin, Sun, D., Luo, M.L., Wu, W., Wang, G.X., 2017. Dual tumor-targeted poly(lactic-co-glycolic acid)–polyethylene glycol–folic acid nanoparticles: A novel biodegradable nanocarrier for secure and efficient antitumor drug delivery. Int. J. Nanomedicine 12, 5745–5760. https://doi.org/10.2147/IJN.S136488

Chiappetta, D.A., Degrossi, J., Teves, S., D'Aquino, M., Bregni, C., Sosnik, A., 2008. Triclosan-loaded poloxamine micelles for enhanced topical antibacterial activity against biofilm. Eur. J. Pharm. Biopharm. 69, 535–545. https://doi.org/10.1016/j.ejpb.2007.11.021

Damodar, G., Smitha, T., Gopinath, S., Vijayakumar, S., Rao, Y., 2014. An evaluation of hepatotoxicity in breast cancer patients receiving injection doxorubicin. Ann. Med. Health Sci. Res. 4, 74. https://doi.org/10.4103/2141-9248.126619

De Esch, C., Slieker, R., Wolterbeek, A., Woutersen, R., de Groot, D., 2012. Zebrafish as potential model for developmental neurotoxicity testing. A mini review. Neurotoxicol. Teratol. https://doi.org/10.1016/j.ntt.2012.08.006

Duggan, S.T., Keating, G.M., 2011. Pegylated liposomal doxorubicin: a review of its use in metastatic breast cancer, ovarian cancer, multiple myeloma and AIDS-related Kaposi's sarcoma. Drugs 71, 2531–58. https://doi.org/10.2165/11207510-000000000-00000

Fleming, A., Diekmann, H., Goldsmith, P., 2013. Functional Characterisation of

the Maturation of the Blood-Brain Barrier in Larval Zebrafish. PLoS One 8, 1–12. https://doi.org/10.1371/journal.pone.0077548

Gao, C., Tang, F., Gong, G., Zhang, J., Hoi, M.P.M., Lee, S.M.-Y., Wang, R., 2017. pH-responsive prodrug nanoparticles based on a sodium alginate derivative for selective co-release of doxorubicin and curcumin in tumor cells. Nanoscale. https://doi.org/10.1039/C7NR03611F

Gut, P., Reischauer, S., Stainier, D.Y.R., Arnaout, R., 2017. LITTLE FISH, BIG DATA: ZEBRAFISH AS A MODEL FOR CARDIOVASCULAR AND METABOLIC DISEASE. Physiol. Rev. 97, 889–938. https://doi.org/10.1152/physrev.00038.2016

He, J.H., Guo, S.Y., Zhu, F., Zhu, J.J., Chen, Y.X., Huang, C.J., Gao, J.M., Dong, Q.X., Xuan, Y.X., Li, C.Q., 2013. A zebrafish phenotypic assay for assessing drug-induced hepatotoxicity. J. Pharmacol. Toxicol. Methods 67, 25–32. https://doi.org/10.1016/j.vascn.2012.10.003

Huang, C. chen, Chen, P.C., Huang, C.W., Yu, J., 2007. Aristolochic acid induces heart failure in zebrafish embryos that is mediated by inflammation. Toxicol. Sci. 100, 486–494. https://doi.org/10.1093/toxsci/kfm235

Kesler, S.R., Blayney, D.W., 2016. Neurotoxic effects of anthracycline- vs nonanthracycline-based chemotherapy on cognition in breast cancer survivors. JAMA Oncol. 2, 185–192. https://doi.org/10.1001/jamaoncol.2015.4333

Kosoko, A.M., Olurinde, O.J., Akinloye, O.A., 2017. Doxorubicin induced neuro- and cardiotoxicities in experimental rats: Protection against oxidative damage by Theobroma cacao Stem bark. Biochem. Biophys. Reports 10, 303–317. https://doi.org/10.1016/j.bbrep.2017.01.012

Kuznetsov, A. V., Margreiter, R., Amberger, A., Saks, V., Grimm, M., 2011. Changes in mitochondrial redox state, membrane potential and calcium precede mitochondrial dysfunction in doxorubicin-induced cell death. Biochim. Biophys. Acta - Mol. Cell Res. 1813, 1144–1152. https://doi.org/10.1016/j.bbamcr.2011.03.002

Lee, K.Y., Jang, G.H., Byun, C.H., Jeun, M., Searson, P.C., Lee, K.H., 2017. Zebrafish models for functional and toxicological screening of nanoscale drug delivery systems: promoting preclinical applications. Biosci. Rep. 37, BSR20170199. https://doi.org/10.1042/BSR20170199

Li, Y., Miao, X., Chen, T., Yi, X., Wang, R., Zhao, H., Lee, S.M.Y., Wang, X., Zheng, Y., 2017. Zebrafish as a visual and dynamic model to study the transport of nanosized drug delivery systems across the biological barriers. Colloids Surfaces B Biointerfaces 156, 227–235. https://doi.org/10.1016/j.colsurfb.2017.05.022

Lillo, C.R., Calienni, M.N., Gorojod, R.M., Rivas Aiello, M.B., Rodriguez Sartori, D., Prieto, M.J., Alonso, S. del V., Kotler, M.L., Gonzalez, M.C., Montanari, J., 2018. Towards biomedical application of amino-functionalized silicon nanoparticles. Nanomedicine 13, 1349–1370.

Liu, C.W., Xiong, F., Jia, H.Z., Wang, X.L., Cheng, H., Sun, Y.H., Zhang, X.Z., Zhuo, R.X., Feng, J., 2013. Graphene-based anticancer nanosystem and its biosafety evaluation using a zebrafish model. Biomacromolecules 14, 358–366. https://doi.org/10.1021/bm3015297

Mohan, P., Rapoport, N., 2010. Doxorubicin as a molecular nanotheranostic agent: Effect of doxorubicin encapsulation in micelles or nanoemulsions on the ultrasound-mediated intracellular delivery and nuclear trafficking. Mol.

Pharm. 7, 1959–1973. https://doi.org/10.1021/mp100269f
Moretton, M.A., Glisoni, R.J., Chiappetta, D.A., Sosnik, A., 2010. Molecular implications in the nanoencapsulation of the anti-tuberculosis drug rifampicin within flower-like polymeric micelles. Colloids Surfaces B Biointerfaces 79, 467–479. https://doi.org/10.1016/j.colsurfb.2010.05.016
Moretton, M.A., Taira, C., Flor, S., Bernabeu, E., Lucangioli, S., Höcht, C., Chiappetta, D.A., 2014. Novel nelfinavir mesylate loaded d-α-tocopheryl polyethylene glycol 1000 succinate micelles for enhanced pediatric anti HIV therapy: In vitro characterization and in vivo evaluation. Colloids Surfaces B Biointerfaces 123, 302–310. https://doi.org/10.1016/j.colsurfb.2014.09.031
Moruno-Manchon, J.F., Uzor, N.E., Kesler, S.R., Wefel, J.S., Townley, D.M., Nagaraja, A.S., Pradeep, S., Mangala, L.S., Sood, A.K., Tsvetkov, A.S., 2018. Peroxisomes contribute to oxidative stress in neurons during doxorubicin-based chemotherapy. Mol. Cell. Neurosci. 86, 65–71. https://doi.org/10.1016/j.mcn.2017.11.014
Neophytou, C.M., Constantinou, C., Papageorgis, P., Constantinou, A.I., 2014. D-alpha-tocopheryl polyethylene glycol succinate (TPGS) induces cell cycle arrest and apoptosis selectively in Survivin-overexpressing breast cancer cells. Biochem. Pharmacol. 89, 31–42. https://doi.org/10.1016/j.bcp.2014.02.003
Ng, A.N.Y., De Jong-Curtain, T.A., Mawdsley, D.J., White, S.J., Shin, J., Appel, B., Dong, P.D.S., Stainier, D.Y.R., Heath, J.K., 2005. Formation of the digestive system in zebrafish: III. Intestinal epithelium morphogenesis. Dev. Biol. 286, 114–135. https://doi.org/10.1016/j.ydbio.2005.07.013
O'Brien, M.E.R., Wigler, N., Inbar, M., Rosso, R., Grischke, E., Santoro, A., Catane, R., Kieback, D.G., Tomczak, P., Ackland, S.P., Orlandi, F., Mellars, L., Alland, L., Tendler, C., 2004. Reduced cardiotoxicity and comparable efficacy in a phase III trial of pegylated liposomal doxorubicin HCl (CAELYX™/Doxil®) versus conventional doxorubicin for first-line treatment of metastatic breast cancer. Ann. Oncol. 15, 440–449. https://doi.org/10.1093/annonc/mdh097
Owen, S.C., Chan, D.P.Y., Shoichet, M.S., 2012. Polymeric micelle stability. Nano Today. https://doi.org/10.1016/j.nantod.2012.01.002
Raldúa, D., Piña, B., 2014. *In vivo* zebrafish assays for analyzing drug toxicity. Expert Opin. Drug Metab. Toxicol. 10, 685–697. https://doi.org/10.1517/17425255.2014.896339
Rizk, H.A., Masoud, M.A., Maher, O.W., 2017. Prophylactic effects of ellagic acid and rosmarinic acid on doxorubicin-induced neurotoxicity in rats. J. Biochem. Mol. Toxicol. e21977. https://doi.org/10.1002/jbt.21977
Selderslaghs, I.W.T., Hooyberghs, J., Blust, R., Witters, H.E., 2013. Assessment of the developmental neurotoxicity of compounds by measuring locomotor activity in zebrafish embryos and larvae. Neurotoxicol. Teratol. 37, 44–56. https://doi.org/10.1016/j.ntt.2013.01.003
Sun, C., Zhou, L., Gou, M., Shi, S., Li, T., Lang, J., 2016. Improved antitumor activity and reduced myocardial toxicity of doxorubicin encapsulated in MPEG-PCL nanoparticles. Oncol. Rep. 35, 3600–3606. https://doi.org/10.3892/or.2016.4748
Yang, F., Chen, Z., Pan, J., Li, X., Feng, J., Yang, H., 2011. An integrated microfluidic array system for evaluating toxicity and teratogenicity of drugs on embryonic zebrafish developmental dynamics. Biomicrofluidics 5.

https://doi.org/10.1063/1.3605509

Yao, Y., Sun, S., Fei, F., Wang, J., Wang, Y., Zhang, R., Wu, J., Liu, L., Liu, X., Cui, Z., Li, Q., Yu, M., Dang, Y., Wang, X., 2017. Screening in larval zebrafish reveals tissue-specific distribution of fifteen fluorescent compounds. Dis. Model. Mech. 10, 1155–1164. https://doi.org/10.1242/dmm.028811

Zhang, Z., Tan, S., Feng, S.S., 2012. Vitamin E TPGS as a molecular biomaterial for drug delivery. Biomaterials. https://doi.org/10.1016/j.biomaterials.2012.03.046

Zhao, H., Li, Q., Hong, Z., 2016. Paclitaxel-loaded mixed micelles enhance ovarian cancer therapy through extracellular pH-triggered PEG detachment and endosomal escape. Mol. Pharm. 13, 2411–2422. https://doi.org/10.1021/acs.molpharmaceut.6b00164

Zhou, T., Dong, Q., Shen, Y., Wu, W., Wu, H., Luo, X., Liao, X., Wang, G., 2016. PEG-b-PCL polymeric nano-micelle inhibits vascular angiogenesis by activating p53-dependent apoptosis in zebrafish. Int. J. Nanomedicine 11, 6517–6531. https://doi.org/10.2147/IJN.S112658

Zou, D., Wang, W., Ren, P., Wang, B., Wang, G., Wang, Y., 2017. Penetration of blood – brain barrier and antitumor activity and nerve repair in glioma by doxorubicin- loaded monosialoganglioside micelles system. Int. J. Nanomedicine 12, 4879–4889. https://doi.org/10.2147/IJN.S138257

Figures

Graphical abstract

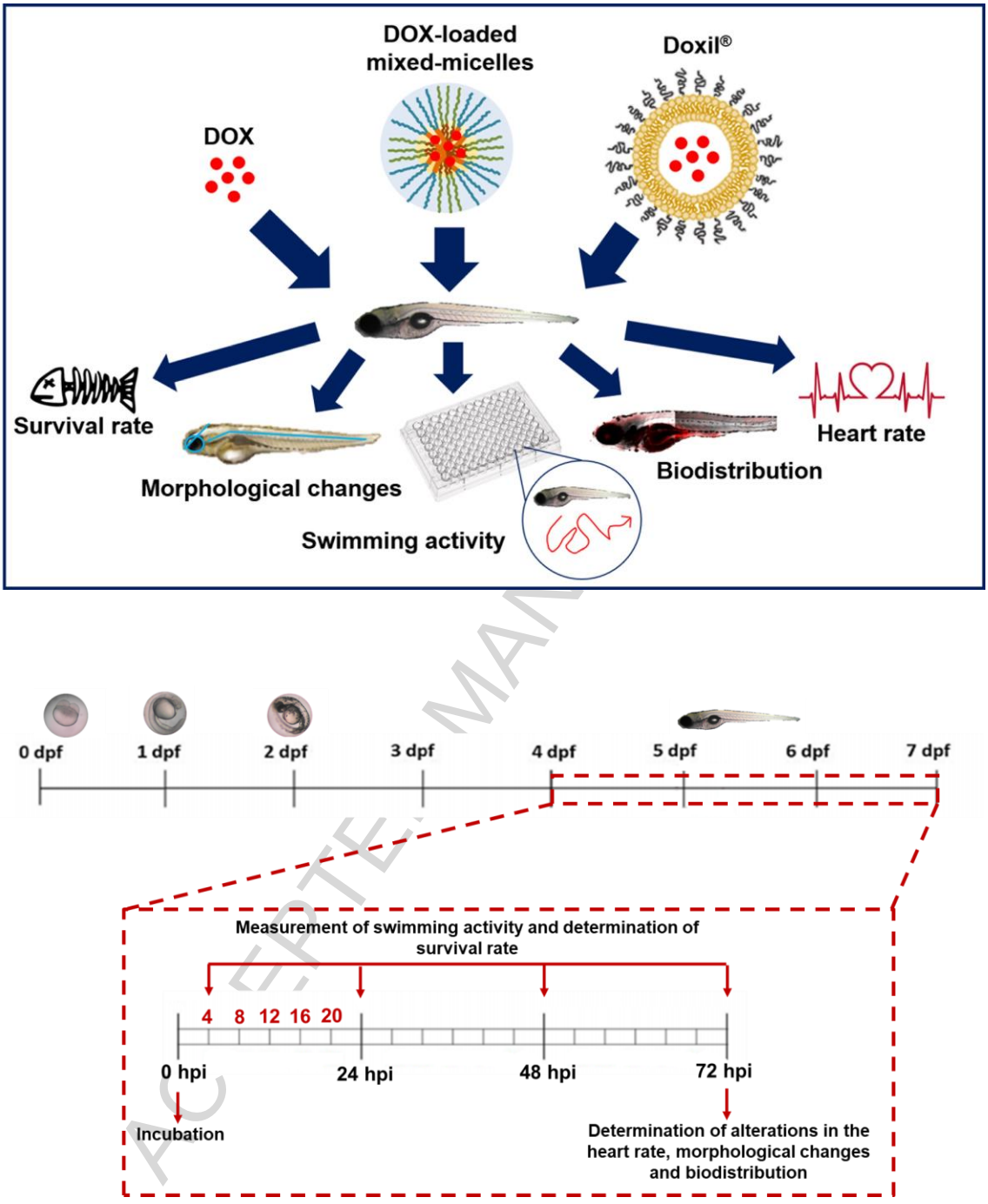

Fig. 1 Timeline of zebrafish development in dpf. The inset shows the time in which determinations were carried out.

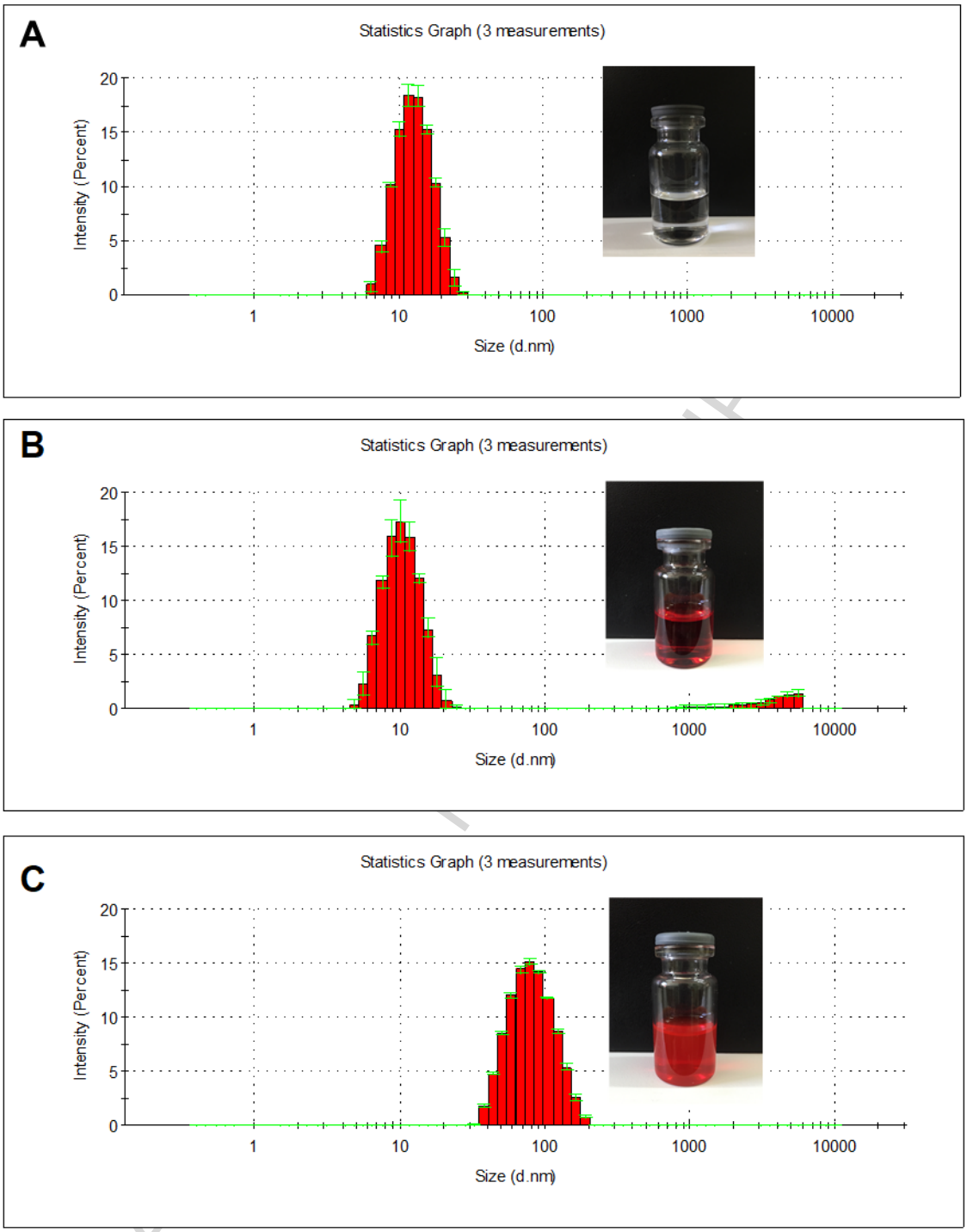

Fig. 2 DLS size distribution of DOX-free mixed micelles (a); DOX-loaded mixed micelles (b) and Doxil® (c). Photo inset: Macroscopic aspect of each nanoformulation.

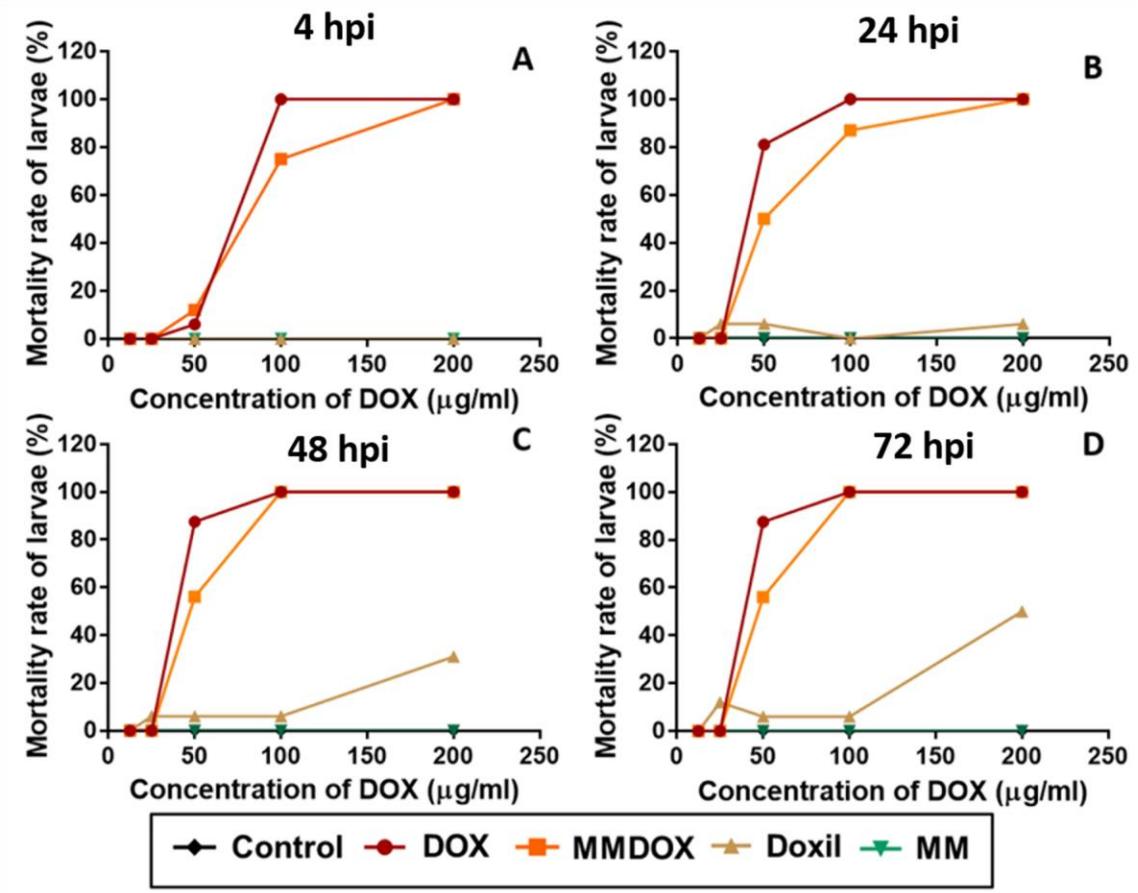

Fig. 3 Percent of mortality rate of larvae after 4 hpi (a), 24 hpi (b), 48 hpi (c) and 72 hpi (d), treated with DOX, DOX-loaded mixed micelles (MMDOX), Doxil®, DOX-free mixed micelles (MM), and E3 medium as control at 4 dpf (n=8 in duplicate). In the case of MM, the concentration tested corresponded to the concentration of polymers in the DOX-loaded mixed micelles.

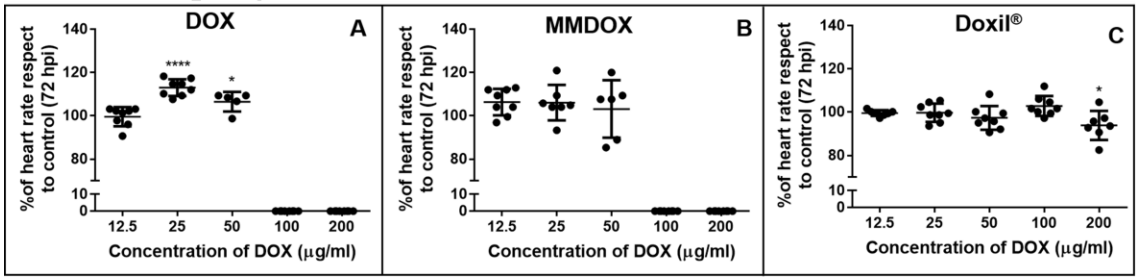

Fig. 4 Percent of heart rate respect to the untreated control of larvae after 72 hpi treated with free DOX (a), MMDOX (b) and Doxil® (c) at 4 dpf (n=4 in duplicate). Data are shown as mean ± SD. Statistical analysis was performed

by ANOVA and the test of Dunnett, comparing all samples against the control (*p < 0.01, ****p < 0.0001).

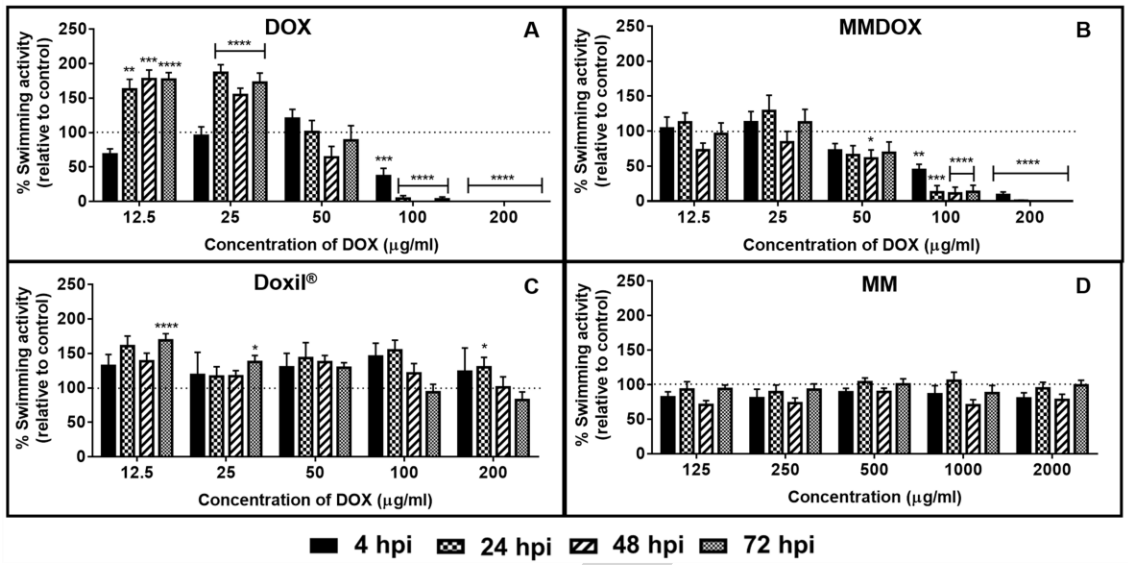

Fig. 5 Percentage of spontaneous swimming activity respect to the control (untreated larvae) at 4, 24, 48 and 72 hpi of larvae exposed to different concentrations of DOX (a), MMDOX (b), Doxil® (c) and MM (d). Data are shown as mean ± SEM (n=8 in triplicate). Activity events were recorded for independent triplicates at room temperature with an automated infrared system. Statistical analysis was performed by ANOVA and the test of Dunnett comparing all samples to the control (* p < 0.05, ** p < 0.01, *** p < 0.001, **** p < 0.0001).

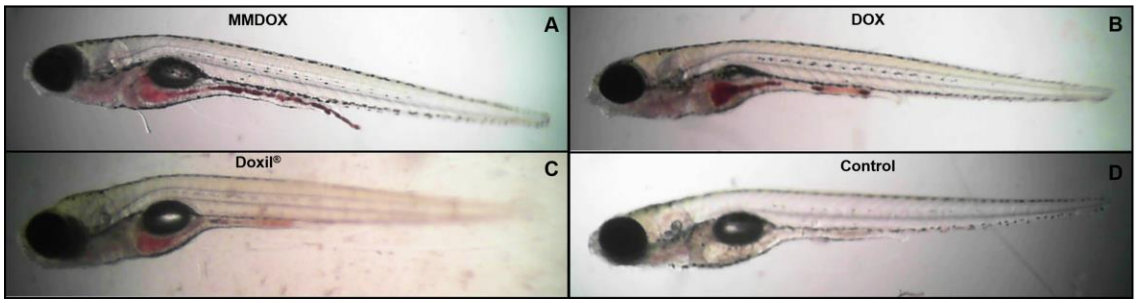

Fig. 6 Images of live zebrafish larvae of 7 dpf (4x) after 72 hpi immobilized in sodium carboxymethylcellulose: MMDOX (50 μg/ml of DOX) (a), DOX (50 μg/ml of DOX) (b), Doxil® (50 μg/ml of DOX) (c) and control (non-treated) (d). Yellow arrows indicate the location of DOX in the lumen of the gut.

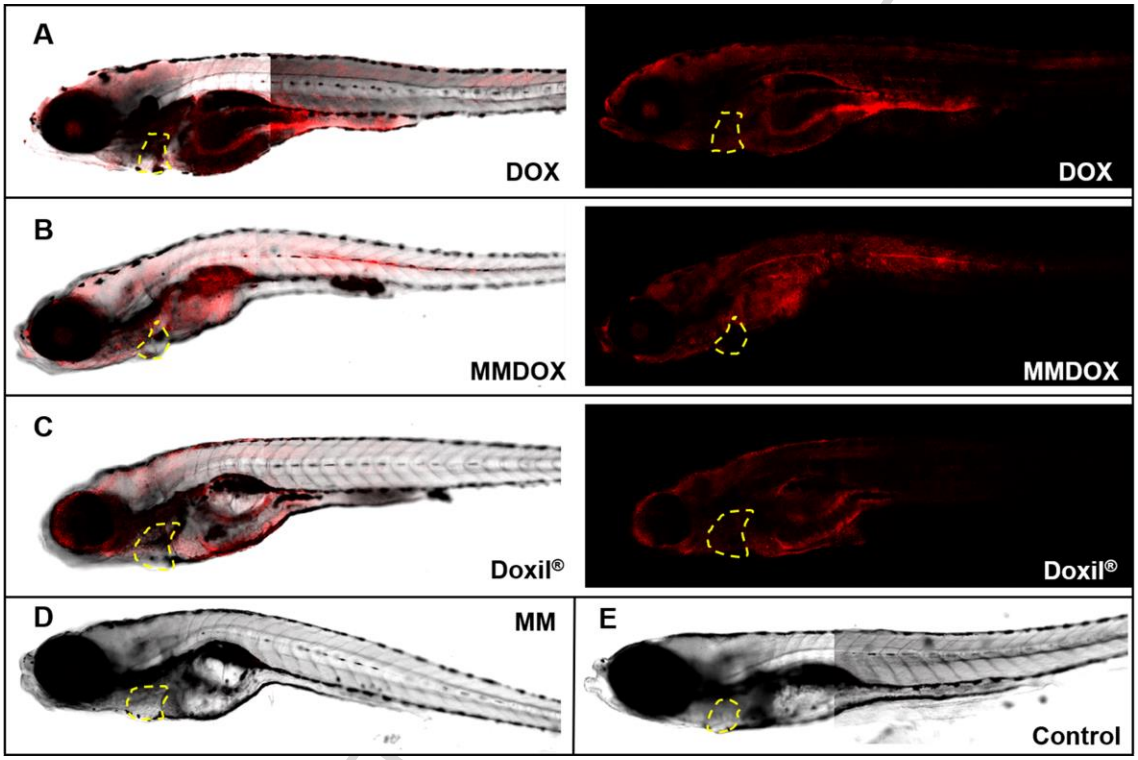

Fig. 7 CLSM of fixed zebrafish larvae of 7 dpf (10x, and digital zoom 1x) after 72 hpi: DOX (a), MMDOX (b), Doxil® (c), MM (d) and control (e). For (a), (b) and (c) the left image corresponds to the merge between confocal (the right one) and the DIC images (non-confocal). No fluorescence was detected for the controls and larvae treated with MM. Yellow dashes indicate the position of the heart, the main target organ of the DOX.

Table

Table 1. Morphological changes on larvae of 7 dpf after 72 hpi treated with free DOX and DOX-loaded mixed micelles (MMDOX). The percentage of larvae with adverse effects was scored as 80-100% (++++), 60-80% (+++), 30-60% (++), 10-30% (+) and 0-10% (-) (n=8).

	12.5 µg/ml[1]		25 µg/ml[1]		50 µg/ml[1]	
	DOX[2]	MMDOX[3]	DOX[2]	MMDOX[3]	DOX[2]	MMDOX[3]
Uninflated swim bladder	+	-	+++	++	++++	++
Arched body	-	-	-	+	+	+
Ulcerated tissue	-	-	-	-	+	-
Pericardial edema	-	-	-	-	-	-

[1] Concentration of free and encapsulated DOX
[2] Free doxorubicin
[3] DOX-loaded mixed micelles

Highlights:

- The *in vivo* toxicity of three DOX formulations was studied on a zebrafish model.
- DOX-loaded mixed micelles were less cardiotoxic than free DOX.
- DOX-loaded mixed micelles presented less morphological alterations than free DOX.
- DOX-loaded mixed micelles exhibited lower neurotoxic effects than free DOX.
- The encapsulation of DOX into mixed micelles reduced the toxic effects of free DOX.

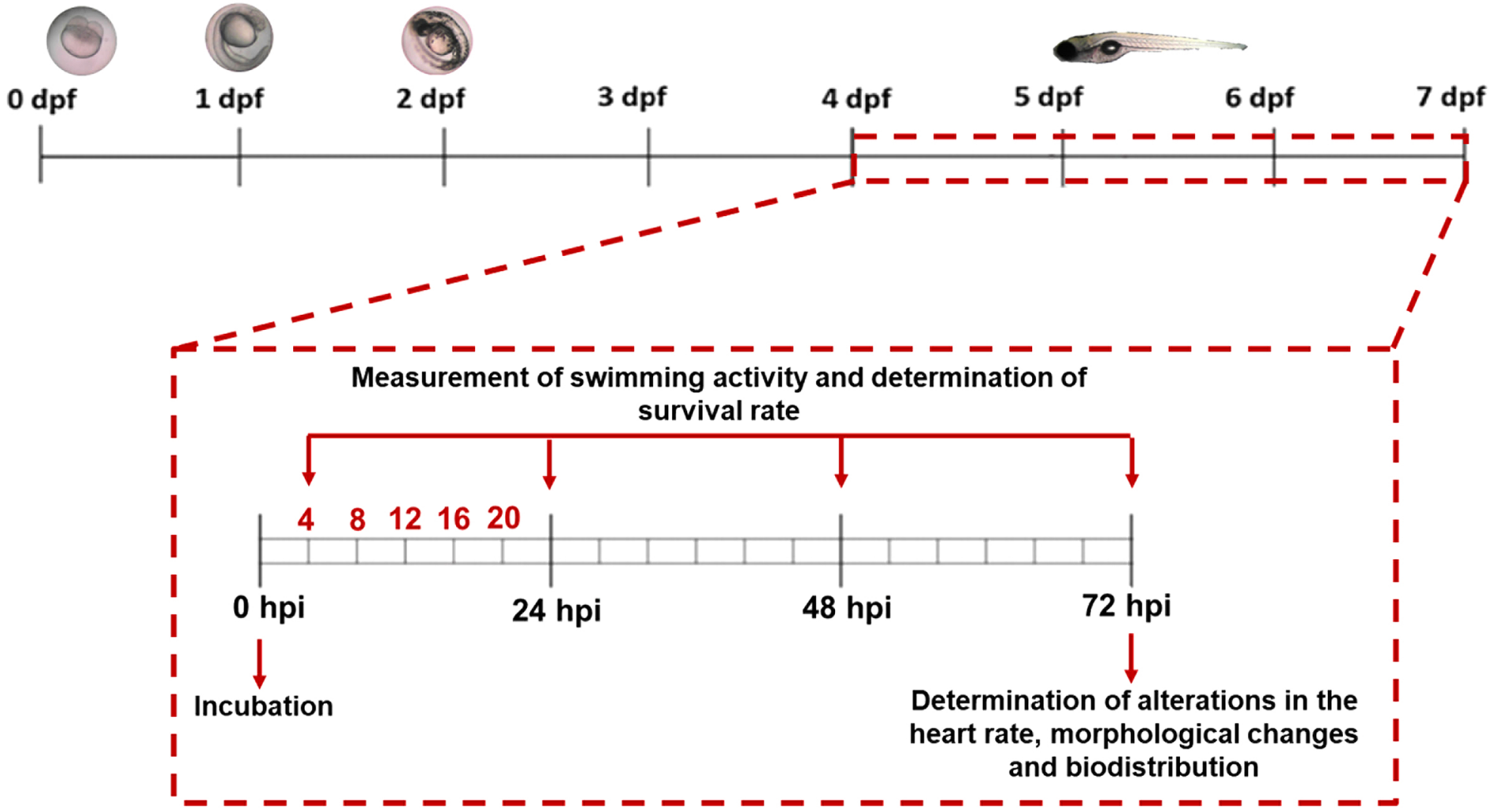
0 dpf
1 dpf
2 dpf
3 dpf
4 dpf
5 dpf
6 dpf
7 dpf
Measurement of swimming activity and determination of survival rate
4 8 12 16 20
0 hpi
24 hpi
48 hpi
72 hpi
Incubation
Determination of alterations in the heart rate, morphological changes and biodistribution

Figure 1

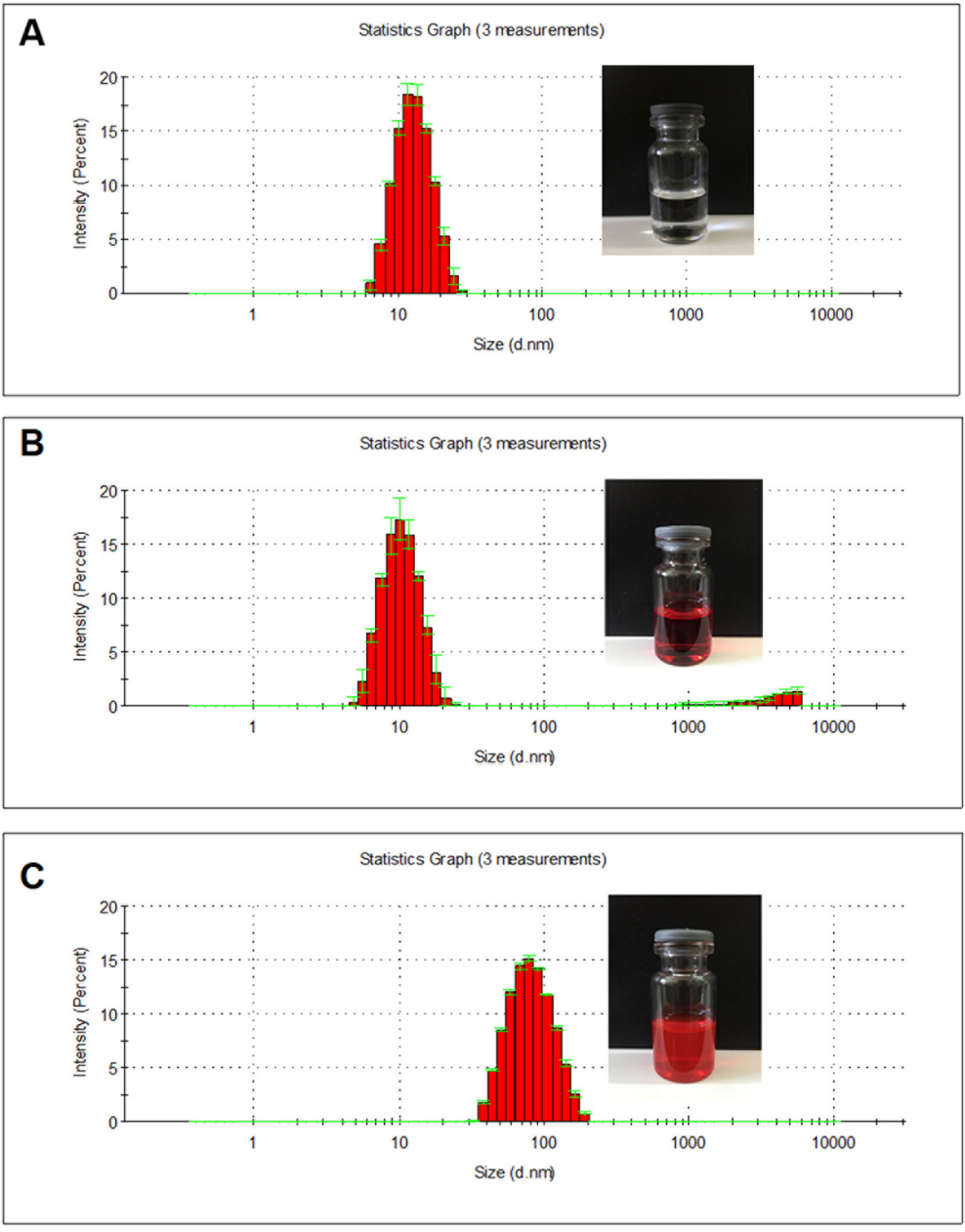
A
Statistics Graph (3 measurements)
Intensity (Percent)
20
15
10
5
0
1
10
100
1000
10000
Size (d.nm)
B
Statistics Graph (3 measurements)
Intensity (Percent)
20
15
10
5
0
1
10
100
1000
10000
Size (d.nm)
C
Statistics Graph (3 measurements)
Intensity (Percent)
20
15
10
5
0
1
10
100
1000
10000
Size (d.nm)

Figure 2

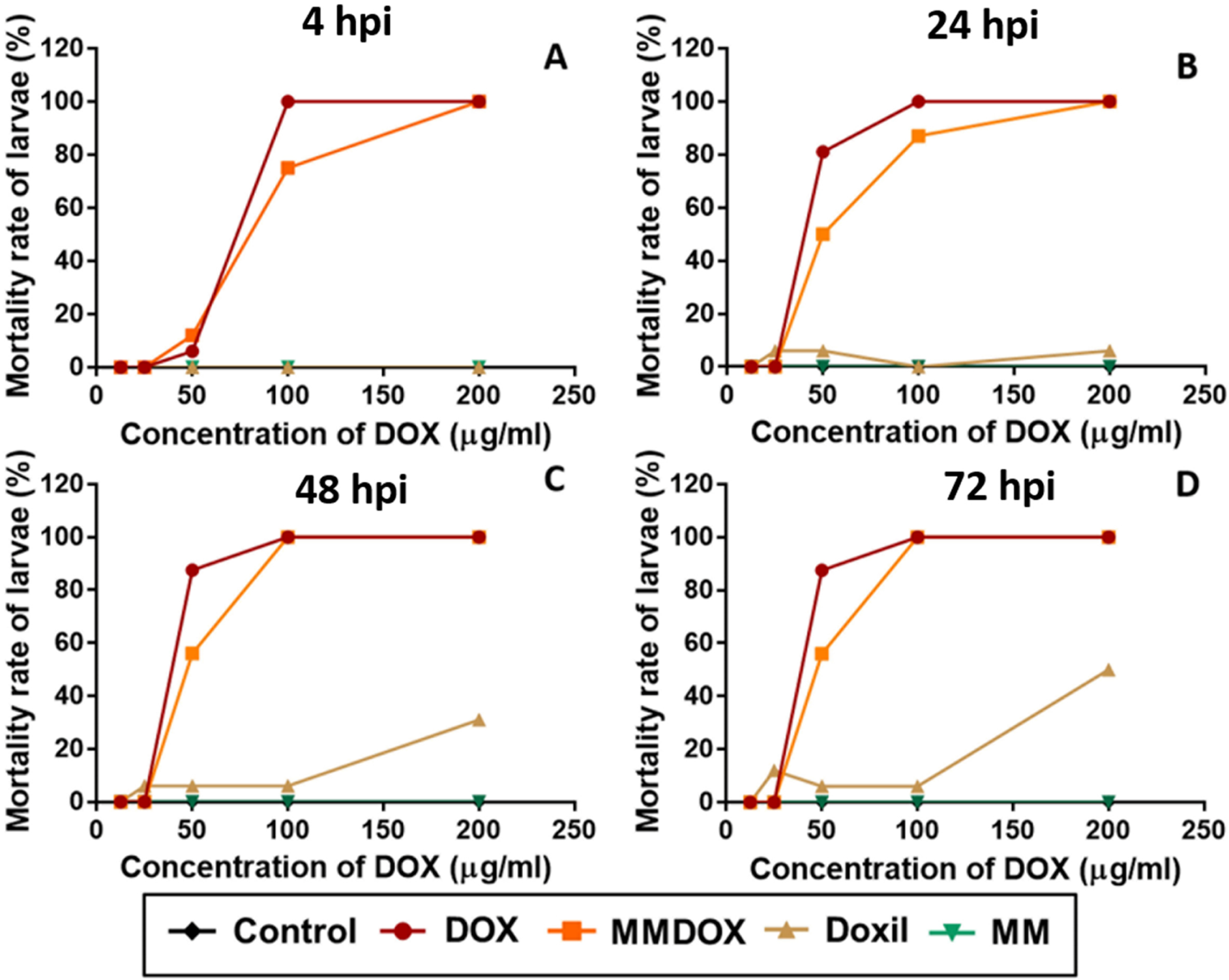
4 hpi
A
24 hpi
B
48 hpi
C
72 hpi
D
Mortality rate of larvae (%)
Concentration of DOX (μg/ml)
0
20
40
60
80
100
120
0
50
100
150
200
250
Control
DOX
MMDOX
Doxil
MM

Figure 3

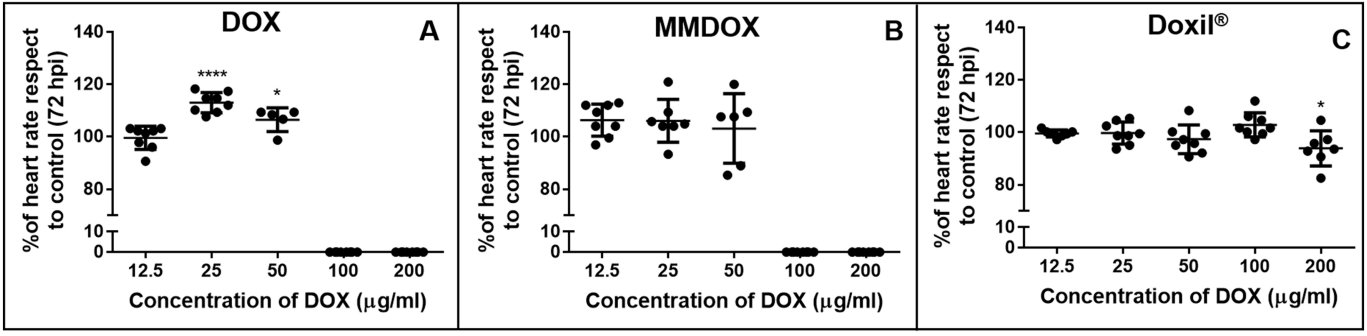
DOX
A
%of heart rate respect to control (72 hpi)
140
120
100
80
10
0
****
*
12.5
25
50
100
200
Concentration of DOX (μg/ml)
MMDOX
B
%of heart rate respect to control (72 hpi)
Concentration of DOX (μg/ml)
Doxil®
C
%of heart rate respect to control (72 hpi)
*
Concentration of DOX (μg/ml)

Figure 4

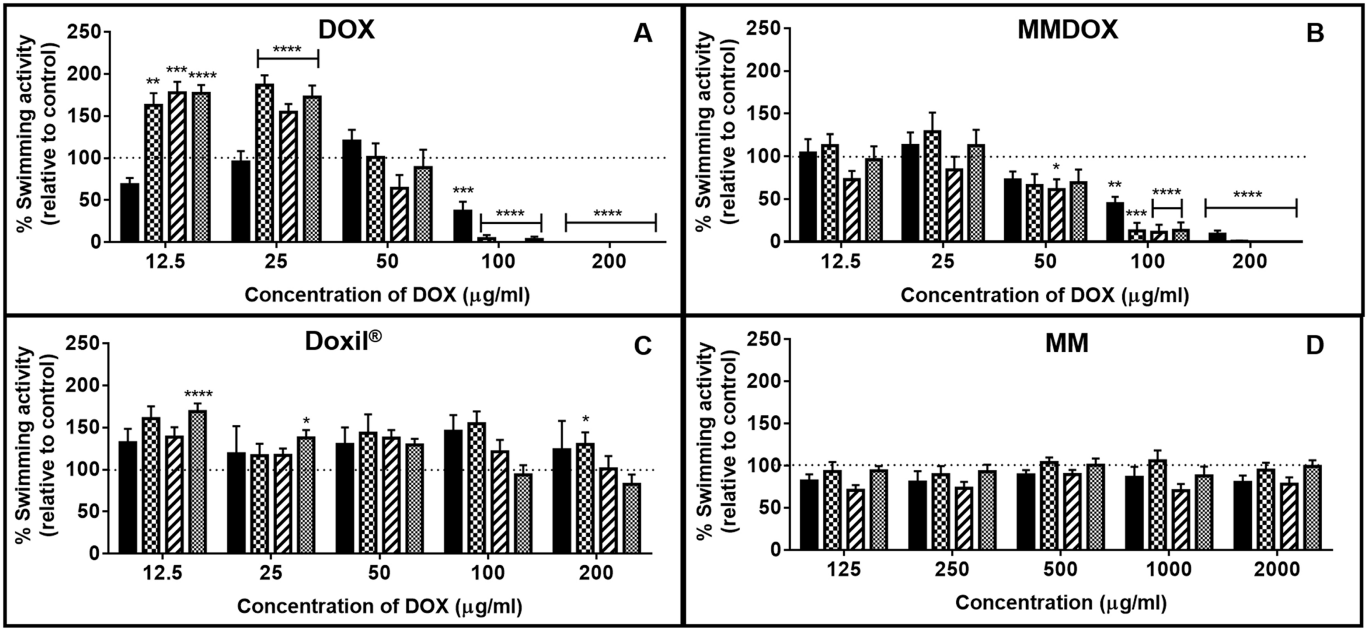
DOX
A
% Swimming activity (relative to control)
250
200
150
100
50
0
12.5
25
50
100
200
Concentration of DOX (μg/ml)
MMDOX
B
Doxil®
C
MM
D
125
250
500
1000
2000
Concentration (μg/ml)
4 hpi
24 hpi
48 hpi
72 hpi

Figure 5

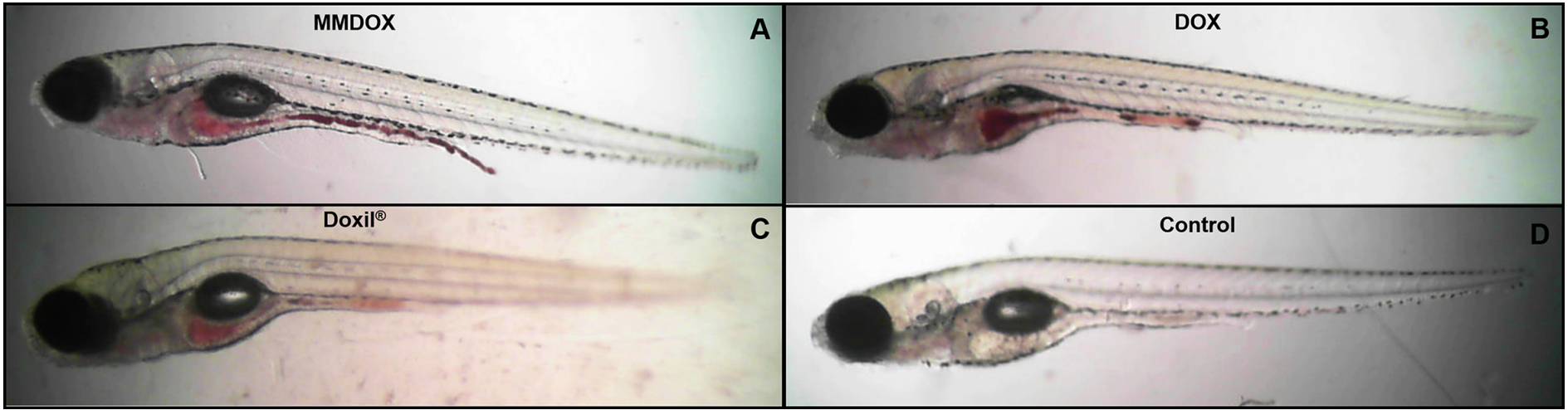

Figure 6

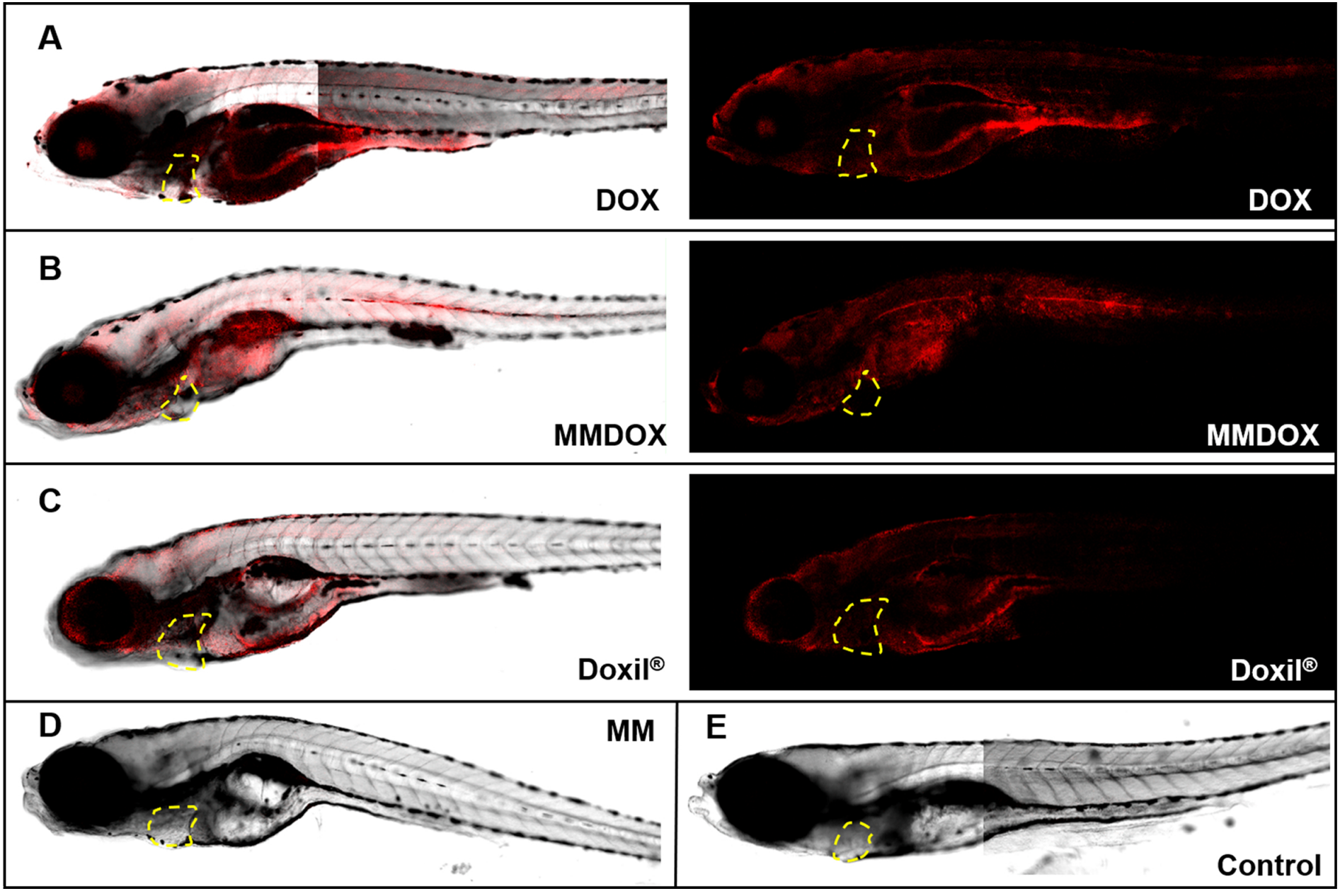

Figure 7